JCTC Journal of Chemical Theory and Computation

Article

pubs.acs.org/JCTC

Quantum Effects in Cation Interactions with First and Second Coordination Shell Ligands in Metalloproteins

Van Ngo,[∇,†] Mauricio C. da Silva,[∇,‡] Maximilian Kubillus,[∇,§,∥] Hui Li,[⊥] Benoît Roux,[⊥] Marcus Elstner,[§] Qiang Cui,[*,∥] Dennis R. Salahub,[*,‡] and Sergei Yu. Noskov[*,†]

[†]Centre for Molecular Simulation and Department of Biological Sciences, University of Calgary, Calgary, Alberta, Canada T2N 1N4

[‡]Centre for Molecular Simulation, Institute for Quantum Science and Technology and Department of Chemistry, University of Calgary, Calgary, Alberta, Canada T2N 1N4

[§]Institute of Physical Chemistry, Karlsruhe Institute of Technology, Kaiserstr. 12, 76021 Karlsruhe, Germany

[∥]Department of Chemistry, University of Wisconsin—Madison, Madison, Wisconsin 53706, United States

[⊥]Department of Biochemistry and Molecular Biology, University of Chicago, Chicago, Illinois 60637, United States

Supporting Information

ABSTRACT: Despite decades of investigations, the principal mechanisms responsible for the high affinity and specificity of proteins for key physiological cations K^+, Na^+, and Ca^{2+} remain a hotly debated topic. At the core of the debate is an apparent need (or lack thereof) for an accurate description of the electrostatic response of the charge distribution in a protein to the binding of an ion. These effects range from partial electronic polarization of the directly ligating atoms to long-range effects related to partial charge transfer and electronic delocalization effects. While accurate modeling of cation recognition by metalloproteins warrants the use of quantum-mechanics (QM) calculations, the most popular approximations used in major biomolecular simulation packages rely on the implicit modeling of electronic polarization effects. That is, high-level QM computations for ion binding to proteins are desirable, but they are often unfeasible, because of the large size of the reactive-site models and the need to sample conformational space exhaustively at finite temperature. Several solutions to this challenge have been proposed in the field, ranging from the recently developed Drude polarizable force-field for simulations of metalloproteins to approximate tight-binding density functional theory (DFTB). To delineate the usefulness of different approximations, we examined the accuracy of three recent and commonly used theoretical models and numerical algorithms, namely, CHARMM C36, the latest developed Drude polarizable force fields, and DFTB3 with the latest 3OB parameters. We performed MD simulations for 30 cation-selective proteins with high-resolution X-ray structures to create ensembles of structures for analysis with different levels of theory, e.g., additive and polarizable force fields, DFTB3, and DFT. The results from DFT computations were used to benchmark CHARMM C36, Drude, and DFTB3 performance. The explicit modeling of quantum effects unveils the key electrostatic properties of the protein sites and the importance of specific ion-protein interactions. One of the most interesting findings is that secondary coordination shells of proteins are noticeably perturbed in a cation-dependent manner, showing significant delocalization and long-range effects of charge transfer and polarization upon binding Ca^{2+}.

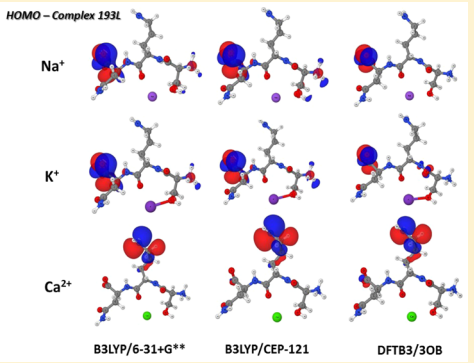

INTRODUCTION

Many cellular processes are critically dependent on the tight control of ionic homeostasis.[1−5] Metal ions play a variety of roles in cellular signaling, nutrients and osmolyte transport, and enzymatic catalysis. Particularly, several proteins have evolved with the ability to bind specific cations, while efficiently excluding competing ions.[6−11] Various factors that alter the binding specificity or affinity of enzymes, such as ion channels or ion-coupled transporters, are known to be associated with a plethora of human diseases, ranging from cardiac arrhythmias to renal dysfunctions to a multitude of neurological disorders.[12−15] Structural, thermodynamic, or functional studies of ion interactions with metalloenzymes are staple items of modern physical biochemistry via molecular simulations, which are playing an ever-increasing role in understanding various mechanisms of cation recognition by protein hosts. One of the key limitations that become more and more apparent is the lack of in-depth understanding of the accuracy of different approximations, which is required in order to define a realistic ion-protein model. Below, we will summarize challenges and limitations relevant to the different levels of theory chosen for this work.

Received: June 4, 2015
Published: September 22, 2015

DOI: 10.1021/acs.jctc.5b00524
J. Chem. Theory Comput. 2015, 11, 4992−5001

The affinity and specificity of protein hosts are fundamentally governed by interactions between the ions and protein ligands. Therefore, the choice of method is pivotal in sampling the conformational space of metalloproteins. The simplest and commonly accepted models are often built on the pairwise-additive assumption used in all of the major biomolecular simulation force fields (FFs)[16−18] (such as CHARMM, NAMD, AMBER, GROMACS). In this assumption, atoms are described as Lennard-Jones particles with simple point-charges. By the virtue of parametrization strategies, it is assumed that quantum effects such as Pauli exclusion, London interactions, etc., are captured implicitly. The transferability of potential parameters developed is assumed. Therefore, the parameter sets that reproduce the quantum mechanics (QM) or experimental observables in a set of model compounds are expected to provide accurate descriptions for biomolecules in different environments. Additive force-fields have been widely successful in studies of biomolecular structure and dynamics with Monte Carlo and molecular dynamics (MD) simulations, many of which have reached millisecond time scales,[19,20] thus allowing a connection of simulations to the realm of biochemical or biophysical experiments.

Nevertheless, there are serious limitations for the additive FFs to accurately capture polarization effects, which are often critical for descriptions of ion binding to protein reactive sites and solvation phenomena, particularly for divalent ions such as Zn^{2+} or Mg^{2+}.[21−23] The additivity assumption breaks down, even for "harder" cations such as Na^+ and Ca^{2+} binding to a variety of sites in metalloproteins.[24] This challenge fueled efforts in the development of next-generation FFs, which approximate more quantum effects, e.g., an extension of the Drude polarizable FF to Na^+, K^+, and Ca^{2+} cations interacting with metalloproteins, while maintaining the transferability, scalability, and modest computational cost.[24] The use of the Drude FF already allows for microsecond simulations with exhaustive sampling of the relevant conformational space.[25] By virtue of the assumptions involved in the creation of the Drude FF (auxiliary particle attached to the heavy atom), it is limited in its ability to describe long-range partial charge transfers.[21] Possible alternatives include either building a full QM model of the metalloprotein *or* resorting to the mixed quantum mechanics/molecular mechanics (QM/MM) treatment of the binding site and its environment.[7,26−30] Both methods are widely popular, but come with a substantial computational cost, especially if the secondary shell ligands are included in the QM region. A promising alternative could possibly be found in the self-consistent-charge density−functional-based tight-binding (SCC-DFTB) approach[31] with the latest extension to include third-order contributions.[32,33] In DFTB3, an electronic energy is perturbed by a series of density fluctuations around a reference density, which is usually taken as a sum of neutral atomic densities. Through a self-consistent solution of the density fluctuations, charge transfers among atoms in a molecule are properly described. A particular advantage of DFTB3 is its computational efficiency, which allows routine sampling of biological systems at the nanoseconds scale in a DFTB3/MM framework for hundreds of atoms.[34−36]

The present study pursues two major goals:

(1) To establish the performance of different approximations (additive and polarizable FFs, DFTB3) in the description of protein−cation interaction energies for a variety of selective metalloenzymes, *and*

(2) To identify the extent of polarization and partial charge propagation in various binding sites accommodating three major physiological cations (Na^+, K^+, and Ca^{2+}).

To achieve our first goal, we examined the interaction energies for a benchmark set of 30 metalloproteins with available high-resolution crystal structures.[24] The proteins perform their function at finite temperatures, where conformational flexibility of the cation binding site is an essential feature of the system.[37] Accurately modeling interactions between metal ions and an ensemble of structures (vs single structure) is the first fundamental step to enable reliable conformational sampling of ion-protein complexes (e.g., via MD or QM/MM-MD schemes). We discuss the accuracy of an additive FF (CHARMM C36), the Drude polarizable FF, and the DFTB3 method in describing the ion−protein interactions in a variety of ion-binding sites with various ligand compositions and local electrostatic environments. Special emphasis will be placed on the evaluation of the DFTB3/3OB parameters.[38] The parameters were developed for a benchmark set containing many small organic molecules. Its applicability to the modeling of ion binding to metalloproteins is yet to be established. The accuracy of the three methods with the above-mentioned parameter sets has been validated against density functional theory (DFT) results.

Next, we evaluated the electrostatic potentials and charge redistribution effects for direct quantification of ion-induced partial-charge transfers and local polarization effects. We chose two model enzymes with different chemical compositions of the first and second coordination shells and cation preferences for a detailed electrostatic analysis. In particular, we focus on hen egg-white lysozyme (PDB: 193L), which is known to bind Na^+ preferentially but allows K^+ and Ca^{2+} binding,[39,40] and in α-amylase (PDB: 2AAA), which binds both Na^+ and Ca^{2+} to form a catalytic triad and is highly selective for Ca^{2+}.[41]

Our results indicate that the inclusion of explicit electronic polarizability and the ability to model long-range partial charge transfer is a necessity for modeling Ca^{2+} binding enzymes. We observed significant differences in the computed interaction energies and the electrostatic maps between detailed (DFT and DFTB3) and approximate models of cation binding to proteins.

METHODOLOGIES

Generation of Protein Conformations. We selected 30 crystal soluble proteins: 10 for each of the cations (K^+, Na^+, or Ca^{2+}). The structural information and PDB[42] entries are listed in Table S1 of the Supporting Information (SI). To create ensembles of conformational states, we solvated the proteins with TIP3P water molecules and 0.15 M of the corresponding salt. We then used NAMD[43] and the CHARMM-36 FF to minimize the structures stepwise and then performed 4-ns equilibration simulations using NPT coupling at a pressure (P) of 1 atm and a temperature (T) of 300 K. All sampled structures display root-mean-square displacement (RMSD) values in the expected range of standard thermal fluctuations.[24] The RMSD values were computed relative to the crystal structures. Next, 20 different conformations of each binding site were extracted. A binding site is defined with a truncation radius of 5.5 Å around the bound ion to include the first (3.0−3.5 Å) and second (5−6 Å) coordination shells of ions. The approach is common in many QM studies of ion binding to proteins.[44] The truncated binding sites have ∼150−300 atoms with 1−6 ligands, several ions, and 2−5 water molecules. The

DOI: 10.1021/acs.jctc.5b00524
J. Chem. Theory Comput. 2015, 11, 4992−5001

properties of the truncated binding sites in the first coordination shell of 3.5 Å are provided in Table 1. These

Table 1. Properties of the Ion-Binding Sites Identified from the Crystal Structures[a]

	Types of Oxygen Atoms[b]					
PDB	OH	−C═O	COO^-	H_2O	extra ion	net charge (|e|)
			K^+ Ion			
1J5Y	0	4	0	3	0	1
1JF8	1	5	1	4	0	−1
1NI4	0	5	0	1	0	2
2BFD	1	6	0	1	0	0
1P36	1	1	1	4	0	−1
1LJL	1	5	1	3	0	−1
1TYY	0	5	1	3	0	1
1DTW	1	6	0	1	0	0
1V3Z	0	5	0	0	0	2
4LS7	1	6	1	2	0	1
			Na^+ Ion			
193L	1	4	0	2	0	3
1E43	0	1	6	1	$2Ca^{2+}$	0
1SFQ	0	2	0	5	0	2
1GEN	0	4	0	0	$1Cl^-$	0
3N0U	0	4	0	3	0	3
1L5B	0	5	0	2	0	1
1QNJ	0	5	3	1	0	−1
1QUS	1	1	4	1	0	−3
1S36	0	5	1	0	$1Cl^-$	0
1SK4	1	5	0	1	0	0
			Ca^{2+} Ion			
3LI3	0	4	3	4	0	−1
1BLI	0	1	5	1	$1Na^+$	0
2UUY	0	3	2	2	0	−2
1A4V	0	2	3	2	0	−2
4KTS	0	3	3	2	0	−2
2AAA	0	2	4	3	0	−5
3TZ1	1	1	5	1	0	−2
1EXR	0	1	5	1	0	−1
1RWY	1	1	6	0	0	0
3ICB	0	5	2	1	0	−1

[a]The total charges are summed up over all atoms in the truncated binding sites. Each element (types of oxygen atoms, H_2O, and ions) is counted within a 3.5 Å sphere centered at the bound ion in the 5.5 Å truncated binding sites. [b]OH, −C═O, and COO^- represent hydroxyl, carbonyl, and carboxylate oxygen atoms, respectively.

conformations of the truncated binding sites were then used to compute ion-binding energies, which are equal to the interaction energy between an ion and its surroundings, using the C36, Drude, and DFTB3/3OB parameters. The C36 FF (shortened as C36) was reported in refs 45−47; the Drude FF (shortened as Drude) was recently developed in ref 24; and the DFTB3/3OB parameters were also recently reported in ref 38.

Quantum-Mechanics Computations. In this work, we have used density functional theory (DFT) to assess quantum effects for reduced models of the binding sites. To evaluate an optimal level of DFT for reference to compare the binding energies from the three parameter sets, a quadruple-ζ basis set, 6-311++G(2d,2p),[48−50] and seven different functionals (PBE,[51,52] PW91,[53] BLYP,[54,55] TPSS,[56] B3LYP,[57] M11,[58] and B2PLYP[59]) were used for two small protein-ion complexes, which are shown in Figure 1 for 193L and 2AAA interacting

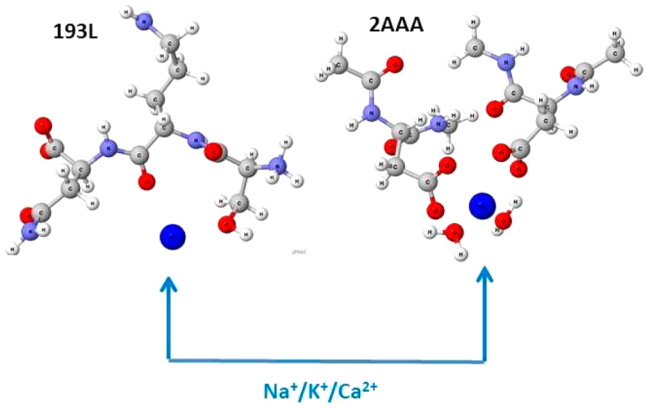

Figure 1. Reduced representations of cation binding sites in 193L and 2AAA with Na^+, K^+, and Ca^{2+}. These simplified structures enable inclusion of the largest basis set for DFT validation and electrostatic analyses. More than 600 structures, which are used for evaluating the different ion-protein models, are fully truncated from the conformational sampling described in the Methodologies section.

with Na^+, K^+, and Ca^{2+}. Using these small complexes, we intend to develop a strategy for identifying electronic perturbations due to different cations in the binding sites. An analysis of the performance of the various methods is provided in the SI to justify the choice of the DFT references. The NWChem v-6.5 package[60] was used for DFT calculations for small ion-protein complexes, while Gaussian 09 Rev. A2[61] was used for all of the larger binding sites. We were interested in assessing an ensemble of structures with single-point computations. To generate ensemble energies, we considered more than 600 truncated structures. All DFT binding energies were corrected for the basis set superposition errors (BSSEs).

To understand the electrostatic environments better, we computed orbital densities, the electron localization function (ELF), and partial charges including Mulliken,[62] ChelpG,[62] and Merz−Kollman[63] for the further-simplified complexes of 193L and 2AAA (Figure 1), using B3LYP/6-31+G(d,p), B3LYP/CEP-121, and DFTB3/3OB. The rationale of computing Mulliken charges is that we can directly compare the results from DFT and DFTB calculations, and observe the possible quantitative changes in protein atoms perturbed by the metal ions. We used Gaussian 09 Rev. A2[61] to generate cube files in association with Multiwfn[64] software to analyze the electronic properties. Jmol software was used to prepare orbital densities, electrostatic maps, and ELF images. All DFTB3/3OB calculations were done with DFTB+ v1.2.2,[65] using the Slater−Koster parameter files recently developed by Elstner and colleagues.[32,66,67] For some small ion-protein complexes, electronic smearing was performed to obtain the convergence of the self-consistent charges (SCC) inside DFTB3/3OB. The Fermi-filling maximum temperature factor for producing the smearing was 70 K, and the Mermin free energy ($E_{tot} - TS_{ele}$) was also used.

RESULTS AND DISCUSSION

On the Choice of Reference for the Full DFT Method. A detailed analysis for the choice of *ab initio* methods is provided in the validation section of the SI; here, we briefly summarize the results. G4 computations[48,68] predict the 20 experimental atomization energies of the small complexes containing Na^+, K^+, and Ca^{2+} with an uncertainty of 2 kcal/mol; thus, G4 is considered to be a good theoretical reference (see

DOI: 10.1021/acs.jctc.5b00524
J. Chem. Theory Comput. 2015, 11, 4992−5001

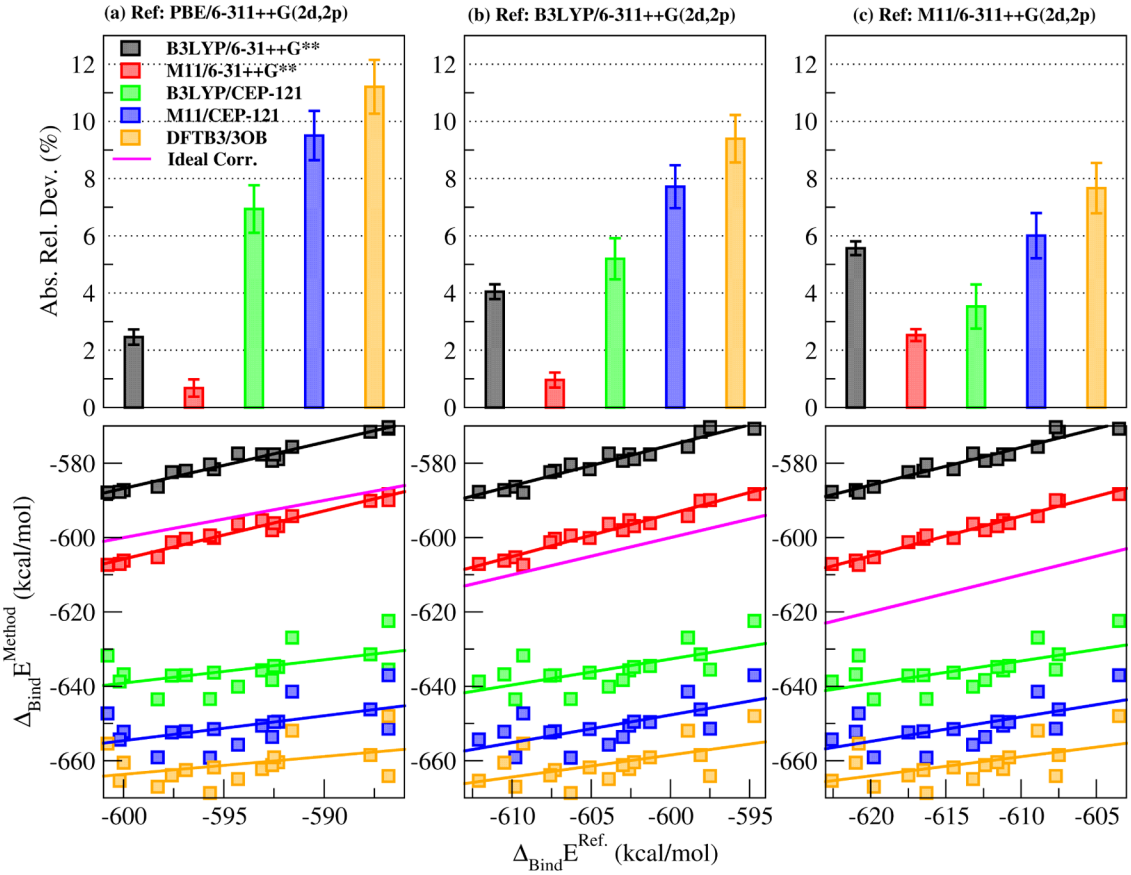

Figure 2. Relative deviation and correlated binding energies ($\Delta_{Bind}E$) for Ca^{2+}-2AAA small model complexes (Figure 1) for different levels of theory, using different electronic structure references: (a) PBE/6-311++G(2d,2p), (b) B3LYP/6-311++G(2d,2p), and (c) M11/6-311++G(2d,2p).

Table S7 in the SI). Tables S8−S25 in the SI show the same accuracy for different types of GGA, hybrid, meta-GGA, and double-hybrid functionals. The DFTB3/3OB results, with respect to those obtained with 6-31+G**, 6-31++G**, and CEP-121, span the same energy range of almost ±20 kcal/mol (see Figures S14 and S15 in the SI). The basis set 6-311++G(2d,2p) is the best for estimating atomization and binding energies, but the computational cost shown in Figure S17 in the SI is prohibitive for large systems. We note that the results obtained with M11 and double-hybrid functionals have the same accuracy as B3LYP; therefore, the choice of B3LYP for a total of more than 600 conformational structures of 150−300 atoms is reasonable, in terms of accuracy and computational cost.

The numerical results for the binding energies for the two small complexes (Figure 1) are collected in Tables S2 and S3. To check the effect of a larger basis set, 6-311++G(2d,2p), interaction energies are compared with the results reported by Li et al.[24] with 6-31++G(d,p) (Tables S2−S5). Table S6 collects the basis-set-dependent differences, in terms of the mean values (μ), standard deviations (σ), and min−max differences (δ). It shows that, for the Na^+-complex, the binding energies are not noticeably different between 6-31++G(d,p) and 6-311++G(2d,2p). The inclusion of extra diffuse and polarization basis functions produces a modest effect at large computational cost. However, for the Ca^{2+}-complex, the average binding energy for B3LYP/6-311++G(2d,2p) is −24.5 kcal mol^{-1}, which is higher than that from B3LYP/6-31++G(d,p) (using M11, it was −15.5 kcal mol^{-1}). This suggests that the addition of extra diffuse and polarization basis functions in the Ca^{2+}-complex can make a critical contribution to the absolute binding energies. The relative deviations and the correlation on the binding energies of Ca^{2+}-2AAA small complex are presented in Figure 2. The similarity between the different levels of method/theory and the reference electronic structures PBE, B3LYP, and M11, using the largest basis set 6-311++G(2d,2p), can be seen in Figure 2.

The long-range polarization effects are expected to be more pronounced in divalent-ion binding sites than in monovalent-ion ones. Therefore, accurate models of divalent-cation binding may demand larger basis sets. For example, we observe that electron densities display a significant perturbation in the second coordination shell of Ca^{2+}, even at distances of 5−6 Å (see below), while the perturbations due to Na^+ and K^+ are considerably smaller. The long-range electrostatic effects induced by Ca^{2+} binding could strongly influence the biophysical and biochemical properties with charge perturbation reaching beyond the first coordination shell. The DFTB3/3OB results are close to those obtained from all-electron or pseudo-potential methods (CEP-121). The pseudo-potential (CEP-121) approximation appears to be reasonable, compared to all-electron calculations for Na^+ or K^+ binding sites. For Ca^{2+} binding sites, DFTB3/3OB or CEP-121 display larger deviations in interactions energies, compared to the full electron calculations, as shown in Tables S2, S3, and S6.

The average deviation of the binding energies for the reduced model of the Ca^{2+}-2AAA complex from computations with DFTB3/3OB and CEP-121 is 25.8 kcal mol^{-1} with the B3LYP functional, but 10.4 kcal mol^{-1} with the M11 functional. The differences between DFTB3/3OB or B3LYP/CEP-121 and all-

DOI: 10.1021/acs.jctc.5b00524
J. Chem. Theory Comput. 2015, 11, 4992−5001

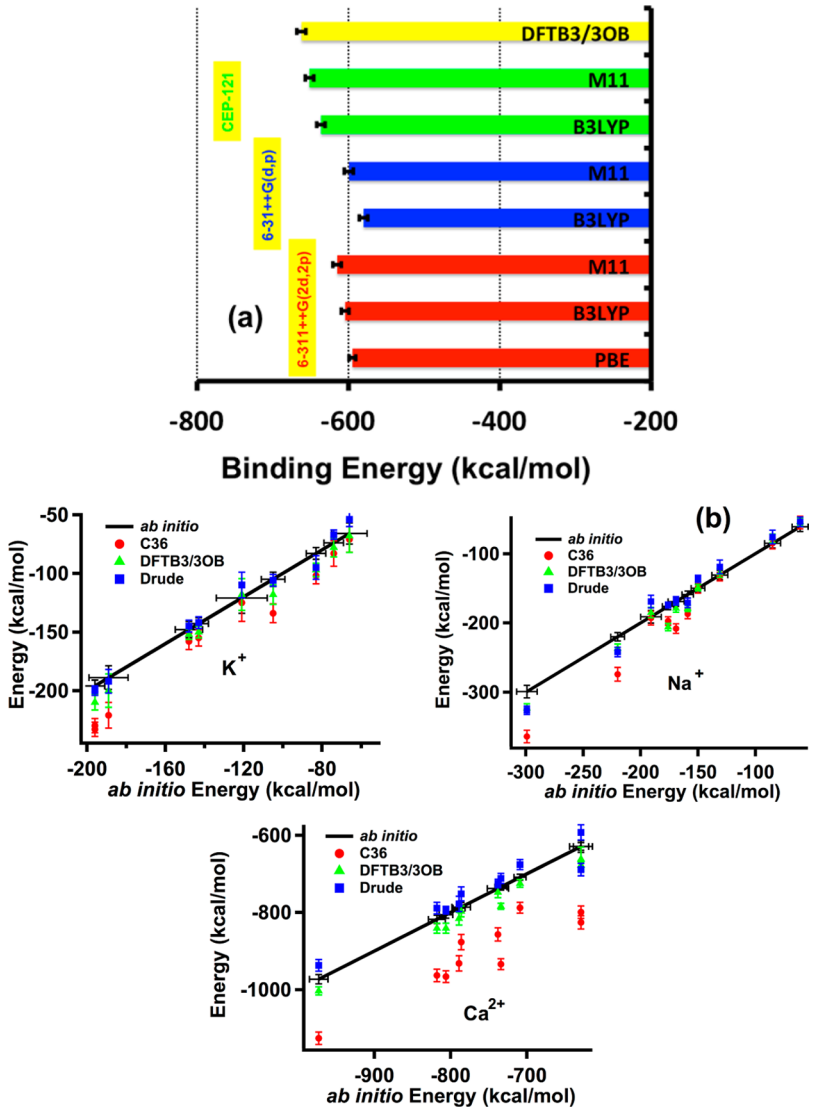

Figure 3. (a) Binding energies from all-electron DFT approximations (numerical values given in Table S5). (b) Binding energies computed by using B3LYP/CEP121, C36, Drude, and DFTB3/3OB calculations for Na^+, K^+, and Ca^{2+} ions.

electron calculations using B3LYP/6-311++G(2d,2p) and M11/6-311++G(2d,2p) are 56.9 kcal mol^{-1} and 47.4 kcal mol^{-1}, respectively. It is important to note that there is a significant variation in the computed interaction energies among all-electron methods themselves. The summary of the results for different all-electron DFT functionals is presented in Figure 3a, suggesting that different functionals and basis sets can vary the binding energies by up to 10%, e.g., between M11/CEP121 and B3LYP/6-311++G(2d,2p). Henceforth, a case was considered as an outlier when exceeding this variation of 10%.

Performance of Three Ion-Protein Models. The protein dynamics due to thermal fluctuations of ions and ligands is essential for enzymatic functions;[37] hence, there is an apparent need for sampling energy surfaces governing ion binding to proteins. To lay a foundation for such sampling, a thorough examination of the major ion−protein models is essential.

The binding energies computed from both Drude and DFTB3/3OB are consistent with the DFT results given the deviations of ≤10%, which returns 8−10 agreement cases for each ionic species. This is not surprising, because the Drude parameter sets were trained to match the DFT interactions.[24] Only two K^+-binding enzymes 1V3Z and 4LS7 in the Drude model display deviations of 18% and 14% in computed interaction energies, relative to all-electron DFT computations. The accuracy of the additive FF (C36) generally becomes poorer when the binding energies are lower than −150 kcal/mol. Therefore, its performance deteriorates noticeably for all of the studied Ca^{2+} binding sites. The interaction energies computed with C36 display an average difference of ∼20%, relative to the DFT results. This indicates serious challenges for reliable simulations of Ca^{2+} binding and/or permeation with additive FFs.

On the other hand, the blind use of the recent DFTB3/3OB parameters developed for small molecules/protein mimetics provides an encouragingly reasonable description for most of the interaction energies. For the K^+-binding proteins, two cases display large deviations (12% for 1TYY and 16% for 4LS7). For the Na^+-proteins, three cases have deviations of 12% (3N0U and 1E43) and 17% (1GEN). Notably, for all of the Ca^{2+}-binding proteins, DFTB3/3OB yields excellent consistency (<8% deviations) with the DFT results. We found that, in two systems (see Table 1) having multiple cation-binding sites, both Drude and DFTB3/3OB accurately reproduce the binding energies (deviations of 5%−10% for 1BLI and 8%−12% for

DOI: 10.1021/acs.jctc.5b00524
J. Chem. Theory Comput. 2015, 11, 4992−5001

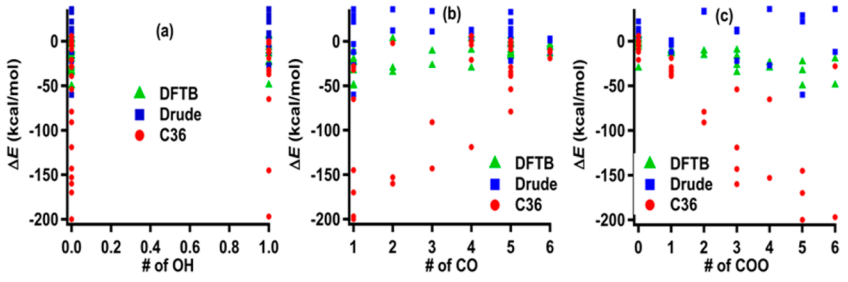

Figure 4. Binding energy difference between the methods and DFT calculations versus oxygen atoms in the binding sites. "OH", "CO", and "COO" represent hydroxyl, carbonyl, and carboxylate oxygen atoms, respectively. These numbers of oxygen atoms are counted within a 3.5-Å sphere centered at the bound ions in the crystal structures (see Table 1 and Table S1 for numerical values).

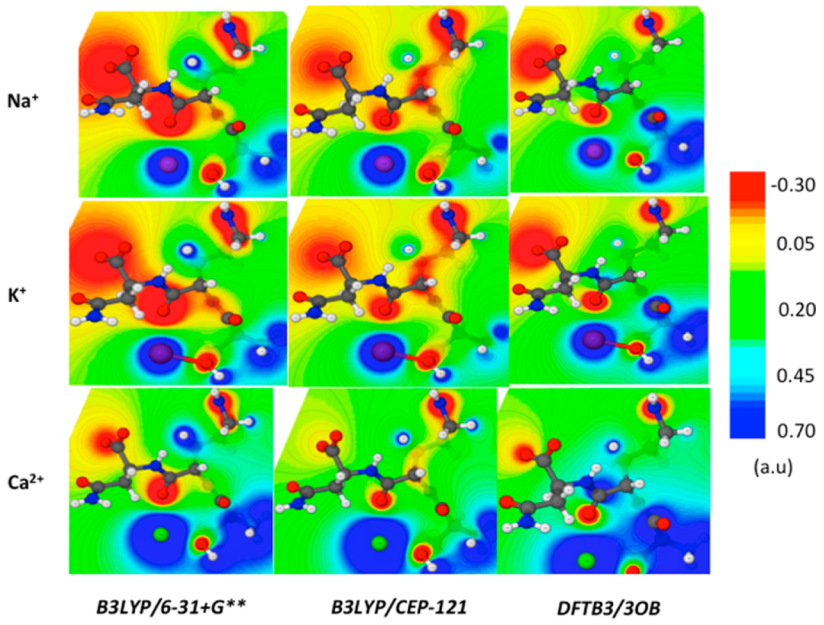

Figure 5. Molecular electrostatic potential (MEP) in atomic units (a.u.) for the simplified 193L complex, whose binding site is interchanged with Na^+, K^+, and Ca^{2+}.

1E43), with respect to the DFT results. This suggests that Drude and DFTB3/3OB can describe multiple-ion interactions with protein ligands, for example, in Na and Ca channels. However, DFTB3/3OB overestimates the binding energy by 17%, with respect to the DFT results for 1GEN with a Cl^- anion present in the structure, but yields an accurate result for 1S36. Drude yields more accurate results than the DFTB3/3OB model for 1GEN, probably because of the fact that the protein−Cl^- interaction was also optimized. In all studied multi-ion systems, the C36 FF yields unreliable results, compared to DFT computations. This finding may have major implications on the recent debate on multi-ionic permeation mechanisms in K^+ and Na^+ ion channels.[7,69]

To understand how different chemical groups affect the accuracies of the methods, we analyze their performance for different binding sites. Figure 4 shows the differences between the binding energies computed by the C36, Drude, DFTB3, and all-electron DFT with the decomposition for the three most common coordinating ligands (i.e., hydroxyls, carbonyls, and carboxylates).

Figure 4a shows that hydroxyl oxygen atoms are unlikely to be the main cause for the discrepancy between C36 and DFT results on the interaction energies. The accurate modeling of the cation−carbonyl interactions already requires some explicit treatment of the polarization effects or charge transfer (Figure 4b). This shows that the performance of the methods improves from C36 to Drude to DFTB3. The need for explicit accounting for QM effects is apparent for all sites with carboxylate groups directly coordinating a bound cation. The performance of C36 deteriorates with the number of carboxylates for all cases except PDB 1E43, which has two Ca^{2+} binding sites. C36 clearly fails to describe the interactions between the ions and the negatively charged carboxylate groups accurately. In contrast, neither Drude nor DFTB3/3OB show a systematic dependence on the types of oxygen atoms or the presence/absence of charged functional groups. Note that an assessment of the actual accuracy with DFT as a benchmark is a challenging task in its own right. For example, different DFT approximations with all-electron basis sets or a pseudopotential, one can get 10−40 kcal/mol differences between the two approximations (see Figure 2), especially for calcium binding sites. Therefore, we are more interested in trends, rather than matching absolute values.

The Extent of the Partial Charge Transfer. Although it represents an important advance, the Drude FF may also be limited in its description of partial charge transfer and long-distance polarization effects.[21] The latter has been proposed to be an essential factor in determining the cation specificity of

DOI: 10.1021/acs.jctc.5b00524
J. Chem. Theory Comput. 2015, 11, 4992−5001

enzymes.[70−72] Dudev and Lim[72] performed a PDB survey for elucidation of the secondary shell ligands that affect cation binding to metalloproteins. They noted that (i) many enzymes have evolved to have tight coupling between first- and second-shell ligands, and (ii) ion−ligand interactions with residues located in secondary shells are often of the same magnitude as those with the directly coordinating functional groups. To shed more light on the local electrostatic environments, we computed the molecular electrostatic potential (MEP) and the electron localization function (ELF) of one binding site (193L), in which we probe local electrostatics in the binding pockets by replacing Na^+ with K^+ and Ca^{2+}. Figure 5 shows that the MEPs for Na^+ and K^+ complexes of lysozyme are very similar. However, the MEP and ELF in the Ca^{2+} complex is quite different from the others.

The effect of the cation binding can be quantified further by assessing partial charges on the protein ligands. Partial charges were calculated with two approximations (ChelpG and MK), which are shown in Figure 6. The perturbations in the partial

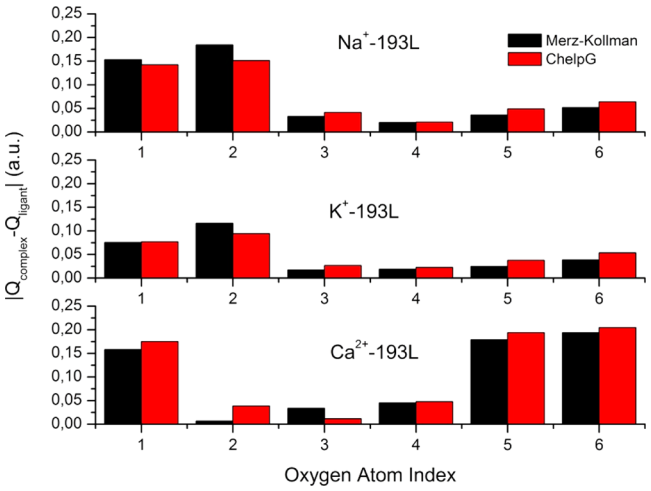

Figure 6. Absolute differences in partial charges of the O atoms in 193L; the index value of 1 indicates the O atom closest to the binding site, and the index value of 6 indicates the O atom furthest from the binding site. Charges were calculated with B3LYP/6-31+G(d,p).

charges of O atoms caused by the binding of Na^+ and K^+ are almost identical and strictly localized to the first-shell ligands. The perturbation of the charges due to Ca^{2+} is very sizable and affects not only the nearest (first coordination shell) atoms, but also significantly the second coordination shells as found in, for instance, ion-sulfur proteins[73] and Ferritin.[74]

To provide additional insight into the underpinnings of the observed perturbations due to the cation binding, we analyzed the highest occupied molecular orbitals (HOMOs) of the complex due to the cation substitution using B3LYP/6-31+G(d,p), B3LYP/CEP-121 and DFTB3/3OB. Both the lowest unoccupied molecular orbital (LUMO) and the HOMO (Figures S8−S12 in the SI) obtained from a few other binding sites are also provided in the SI.

Figure 7 shows the HOMO orbitals for the 193L complex using B3LYP/6-31+G**, B3LYP/CEP-121, and DFTB3/3OB, which are localized near the ions and are more or less identical for Na^+ and K^+-complexes. In sharp contrast, the HOMO orbitals (and, thus, the overall electron densities shown in Figure S13 in the SI) computed by B3LYP for the Ca^{2+}-complex are remarkably different from the other complexes: electrons are found to be transferred through the nearest ligands to delocalize onto the second coordination shell. DFTB3/3OB seems to capture a similar fraction of the electron delocalization[75,76] reported from the DFT calculations. Of course, the amount of charge transfer or delocalization in the various methods is critically dependent on the binding site.[77] For example, the HOMO obtained from DFTB3/3OB in 2AAA (Figure S11) is not as dramatically different from the B3LYP HOMO as from those in Figure 7 and Figure S9. An ELF analysis of the Na^+, K^+, and Ca^{2+} model complexes also indicates that the electronic densities of Na^+ and K^+ give rise to almost the same partial charges of 1|e| when using B3LYP with 6-31+G(d,p) and CEP-121 (Figures S1 and S2), but there is a charge transfer from the ligand to Ca^{2+}, resulting in a partial charge as small as 1.2 |e|.

To illustrate how the electrostatic environments of an entire protein host affects the ion binding affinities, Figure 8 shows the deviations between the binding energies and DFT calculations against the net charges of the truncated binding sites. Consistent with Figure 4c, the electrostatic environments (see Figure 8a) modeled by C36 induce overbinding to the ions, since most of the data points have negative-energy deviations (see Figure 3). In contrast, Figures 8b and 8c simply show random-like data for energy deviations of <17% over many of the electrostatic environments having a net charge of $|q| \leq 5|e|$. In the neutral systems, DFTB3/3OB and Drude sometimes experience difficulties in accurately calibrating the electron densities to have an accuracy of <10%. Therefore, the efficiency of the DFTB3/3OB and Drude FFs for simulating larger systems and longer time scales may be very appealing, because, for most of the studied systems, it appears to be a reasonable tradeoff with only a few outliers, having deviations of 12%−17%, relative to the DFT computations.

CONCLUSIONS

In conclusion, we have benchmarked the accuracy of the nonpolarizable C36 force field (FF), the newly developed Drude polarizable FF, and the DFTB3/3OB method against DFT calculations for effectively describing interactions among 30 enzymatic metalloproteins and cations K^+, Na^+, and Ca^{2+}. We found that, even though C36 can reasonably describe the interactions between the monovalent ions and some proteins (~60% success rate), it fails to accurately reproduce QM trends observed for interactions between Ca^{2+} and all 10 of the proteins. In contrast, the Drude FF and DFTB3/3OB reproduce QM energetics for most of the studied binding sites with various electrostatic environments. Therefore, taking account of polarization effects is crucial for studies of Ca^{2+}-binding sites and is strongly recommended for divalent cations. It also captures the main average trends for all conformations of the Ca^{2+}-complexes very well, although the absolute values of the binding energy may vary somewhat (~10%), compared to higher levels of theory. We provide evidence that this may be due to the approximate treatments of long-range electronic effects. Detailed examination of electron densities shows that, while C36 and Drude FF are unable to sufficiently capture the delocalization effect of electron clouds onto the second coordination shells of divalent ions, DFTB3/3OB provides a reasonable level of accuracy. That is, the electron densities of ligands around Ca^{2+} can be delocalized and, therefore, additional measures for charge-transfer and polarizable effects must be taken and long-range interaction effects and polarization of the electron clouds could be crucial to the accuracy of

DOI: 10.1021/acs.jctc.5b00524
J. Chem. Theory Comput. 2015, 11, 4992−5001

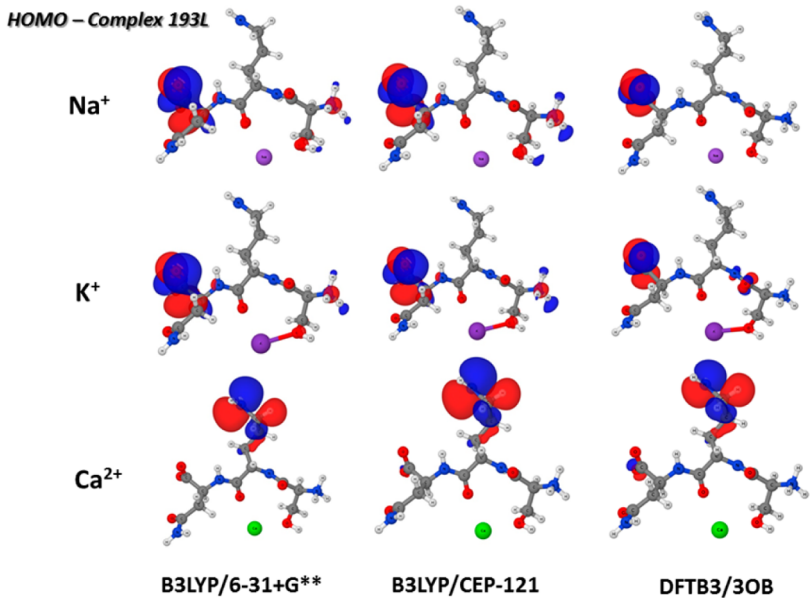

Figure 7. Highest occupied molecular orbital (HOMO) for the 193L complex probed with Na^+, K^+, and Ca^{2+} on its binding site for DFT and DFTB3/3OB.

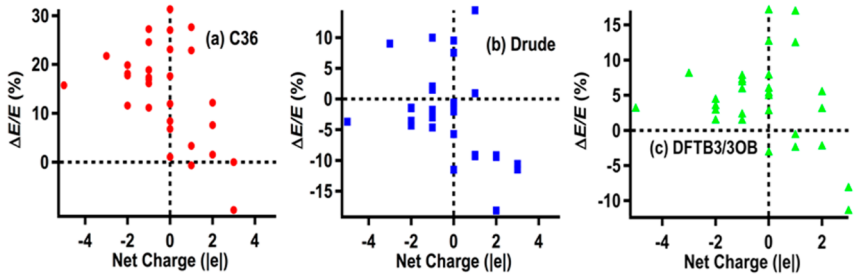

Figure 8. Binding energy deviation ratio ($\Delta E/E$) versus the net charge ($|e|$) of the binding sites for C36, Drude, and DFTB3/3OB.

any biological models. This work is a critical step toward future research that intends to determine the optimal protein structures that result in the largest delocalization effect in divalent-ion binding sites, and reveal how such structures determine the functionalities of biological systems at multiple levels of theory.

■ ASSOCIATED CONTENT

Supporting Information

The Supporting Information is available free of charge on the ACS Publications website at DOI: 10.1021/acs.jctc.5b00524.

Numerical data for the figures shown in the main text, and detailed analysis on the electrostatic properties and the performance of DFT functionals and basis sets (PDF)

■ AUTHOR INFORMATION

Corresponding Authors

*E-mail: cui@chem.wisc.edu (Q. Cui).
*E-mail: dennis.salahub@ucalgary.ca (D. R. Salahub).
*E-mail: snoskov@ucalgary.ca (S. Yu. Noskov).

Author Contributions

[∇]These authors contributed equally to this work.

Notes

The authors declare no competing financial interest.

■ ACKNOWLEDGMENTS

The work in Calgary was supported by the Natural Sciences and Engineering Research Council of Canada (NSERC) (Discovery Grant No. RGPIN-315019 to S.Y.N. and Grant No. RGPIN-10174 to D.R.S.) and Alberta Innovates Technology Futures (AITF) Strategic Chair in BioMolecular Simulations (Centre for Molecular Simulation). S.Y.N. is a Canadian Institute for Health Research New Investigator, and an Alberta Innovates Health Solutions (AIHS) Scholar. V.N. is supported by AIHS Postdoctoral Fellowship. M.K. thanks the Karlsruhe House of Young Scientists (KHYS) for the financial support. Q.C. acknowledges support by the NIH Grant No. R01-GM106443. This work was also supported by the National Science Foundation, through Grant No. GM-072558 awarded to B.R. The computations were enabled by resource allocation grants from Compute Canada (West-Grid HPC), the Laboratory Computing Resource Center (LCRC) of the Argonne National Lab of the United States, and the Extreme Science and Engineering Discovery Environment (XSEDE) network.

■ LIST OF ABBREVIATIONS:

RMSD = root-mean-square displacement
DFT = density functional theory
DFTB = density functional tight binding
FF = force field

DOI: 10.1021/acs.jctc.5b00524
J. Chem. Theory Comput. 2015, 11, 4992−5001

QM/MM = quantum mechanics/molecular mechanics
BSSE = basis set superposition error
ELF = electron localization function
MEP = molecular electrostatic potential
HOMO = highest occupied molecular orbitals
LUMO = lowest unoccupied molecular orbital

REFERENCES

(1) Ueda, E. K. M.; Gout, P. W.; Morganti, L. Current and Prospective Applications of Metal Ion−Protein Binding. *J. Chromatogr. A* **2003**, *988*, 1−23.
(2) Record, M. T.; Anderson, C. F.; Lohman, T. M. Thermodynamic Analysis of Ion Effects on the Binding and Conformational Equilibria of Proteins and Nucleic Acids: The Roles of Ion Association or Release, Screening, and Ion Effects on Water Activity. *Q. Rev. Biophys.* **1978**, *11*, 103−178.
(3) Baldwin, R. L. How Hofmeister Ion Interactions Affect Protein Stability. *Biophys. J.* **1996**, *71*, 2056−2063.
(4) Assche, F. V.; Clijsters, H. Effects of Metals on Enzyme Activity in Plants. *Plant, Cell Environ.* **1990**, *13*, 195−206.
(5) Rembert, K. B.; Paterová, J.; Heyda, J.; Hilty, C.; Jungwirth, P.; Cremer, P. S. Molecular Mechanisms of Ion-Specific Effects on Proteins. *J. Am. Chem. Soc.* **2012**, *134*, 10039−10046.
(6) Roux, B. Computational Electrophysiology: The Molecular Dynamics of Ion Channel Permeation and Selectivity in Atomistic Detail. *Biophys. J.* **2011**, *101*, 755−756.
(7) Roux, B.; Berneche, S.; Egwolf, B.; Lev, B.; Noskov, S. Y.; Rowley, C. N.; Yu, H. B. Ion Selectivity in Channels and Transporters. *J. Gen. Physiol.* **2011**, *137*, 415−426.
(8) Doyle, D. A.; Cabral, J. M.; Pfuetzner, R. A.; Kuo, A. L.; Gulbis, J. M.; Cohen, S. L.; Chait, B. T.; MacKinnon, R. The Structure of the Potassium Channel: Molecular Basis of K^+ Conduction and Selectivity. *Science* **1998**, *280*, 69−77.
(9) Payandeh, J.; Scheuer, T.; Zheng, N.; Catterall, W. A. The Crystal Structure of a Voltage-Gated Sodium Channel. *Nature* **2011**, *475*, 353−358.
(10) Tang, L.; Gamal El-Din, T. M.; Payandeh, J.; Martinez, G. Q.; Heard, T. M.; Scheuer, T.; Zheng, N.; Catterall, W. A. Structural Basis for Ca^{2+} Selectivity of a Voltage-Gated Calcium Channel. *Nature* **2013**, *505*, 56−61.
(11) Rao, L.; Cui, Q.; Xu, X. Electronic Properties and Desolvation Penalties of Metal Ions Plus Protein Electrostatics Dictate the Metal Binding Affinity and Selectivity in the Copper Efflux Regulator. *J. Am. Chem. Soc.* **2010**, *132*, 18092−18102.
(12) Sanguinetti, M. C.; Tristani-Firouzi, M. Herg Potassium Channels and Cardiac Arrhythmia. *Nature* **2006**, *440*, 463−469.
(13) Schwartz, P. J.; et al. Genotype-Phenotype Correlation in the Long-QT Syndrome—Gene-Specific Triggers for Life-Threatening Arrhythmias. *Circulation* **2001**, *103*, 89−95.
(14) Dingledine, R.; Borges, K.; Bowie, D.; Traynelis, S. F. The Glutamate Receptor Ion Channels. *Pharmacol. Rev.* **1999**, *51*, 7−61.
(15) Meisler, M. H.; Kearney, J. A. Sodium Channel Mutations in Epilepsy and Other Neurological Disorders. *J. Clin. Invest.* **2005**, *115*, 2010−2017.
(16) Brooks, B. R.; Bruccoleri, R. E.; Olafson, B. D.; States, D. J.; Swaminathan, S.; Karplus, M. Charmm—A Program for Macromolecular Energy, Minimization, and Dynamics Calculations. *J. Comput. Chem.* **1983**, *4*, 187−217.
(17) Pearlman, D. A.; Case, D. A.; Caldwell, J. W.; Ross, W. S.; Cheatham, T. E.; Debolt, S.; Ferguson, D.; Seibel, G.; Kollman, P. Amber, a Package of Computer-Programs for Applying Molecular Mechanics, Normal-Mode Analysis, Molecular-Dynamics and Free-Energy Calculations to Simulate the Structural and Energetic Properties of Molecules. *Comput. Phys. Commun.* **1995**, *91*, 1−41.
(18) Berendsen, H. J. C.; Vanderspoel, D.; Vandrunen, R. Gromacs—A Message-Passing Parallel Molecular-Dynamics Implementation. *Comput. Phys. Commun.* **1995**, *91*, 43−56.
(19) Shaw, D. E.; et al. Atomic-Level Characterization of the Structural Dynamics of Proteins. *Science* **2010**, *330*, 341−346.
(20) Tozzini, V. Coarse-Grained Models for Proteins. *Curr. Opin. Struct. Biol.* **2005**, *15*, 144−150.
(21) Riahi, S.; Roux, B.; Rowley, C. N. QM/MM Molecular Dynamics Simulations of the Hydration of Mg(II) and Zn(II) Ions. *Can. J. Chem.* **2013**, *91*, 552−558.
(22) Gresh, N.; Claverie, P.; Pullman, A. Theoretical Studies of Molecular Conformation. Derivation of an Additive Procedure for the Computation of Intramolecular Interaction Energies. Comparison with *Ab Initio* SCF Computations. *Theor. Chim. Acta* **1984**, *66*, 1−20.
(23) Li, P.; Merz, K. M., Jr. Taking into Account the Ion-Induced Dipole Interaction in the Nonbonded Model of Ions. *J. Chem. Theory Comput.* **2014**, *10*, 289−297.
(24) Li, H.; Ngo, V.; Da Silva, M. C.; Salahub, D. R.; Callahan, K.; Roux, B.; Noskov, S. Y. Representation of Ion−Protein Interactions Using the Drude Polarizable Force-Field. *J. Phys. Chem. B* **2015**, *119*, 9401−9416.
(25) Huang, J.; Lopes, P. E. M.; Roux, B.; MacKerell, A. D. Recent Advances in Polarizable Force Fields for Macromolecules: Microsecond Simulations of Proteins Using the Classical Drude Oscillator Model. *J. Phys. Chem. Lett.* **2014**, *5*, 3144−3150.
(26) Warshel, A.; Levitt, M. Theoretical Studies of Enzymic Reactions—Dielectric, Electrostatic and Steric Stabilization of Carbonium-Ion in Reaction of Lysozyme. *J. Mol. Biol.* **1976**, *103*, 227−249.
(27) Lev, B.; Roux, B.; Noskov, S. Y. Relative Free Energies for Hydration of Monovalent Ions from QM and QM/MM Simulations. *J. Chem. Theory Comput.* **2013**, *9*, 4165−4175.
(28) Gresh, N.; Pullman, A.; Claverie, P. Cation Ligand Interactions—Reproduction of Extended Basis Set *ab initio* SCF Computations by the SIBFA-2 Additive Procedure. *Int. J. Quantum Chem.* **1985**, *28*, 757−771.
(29) Pullman, A.; Gresh, N.; Daudey, J. P.; Moskowitz, J. W. Use of Pseudopotentials for Study of Cation-Ligand and Intermolecular Interactions. *Int. J. Quantum Chem.* **1977**, *12*, 501−507.
(30) Pullman, A.; Berthod, H.; Gresh, N. Cation-Ligand Interactions—*Ab initio* SCF Studies of Binding Properties of Alkali, Alkaline-Earth, and Ammonium-Ions. *Int. J. Quantum Chem.* **1976**, *10*, 59−76.
(31) Elstner, M.; Porezag, D.; Jungnickel, G.; Elsner, J.; Haugk, M.; Frauenheim, T.; Suhai, S.; Seifert, G. Self-Consistent-Charge Density-Functional Tight-Binding Method for Simulations of Complex Materials Properties. *Phys. Rev. B: Condens. Matter Mater. Phys.* **1998**, *58*, 7260−7268.
(32) Gaus, M.; Cui, Q. A.; Elstner, M. Dftb3: Extension of the Self-Consistent-Charge Density-Functional Tight-Binding Method (SCC-DFTB). *J. Chem. Theory Comput.* **2011**, *7*, 931−948.
(33) Kaminski, S.; Giese, T. J.; Gaus, M.; York, D. M.; Elstner, M. Extended Polarization in Third-Order SCC-DFTB from Chemical-Potential Equalization. *J. Phys. Chem. A* **2012**, *116*, 9131−9141.
(34) Seifert, G.; Joswig, J. O. Density-Functional Tight Binding—An Approximate Density-Functional Theory Method. *Wiley Interdiscip. Rev.: Comput. Mol. Sci.* **2012**, *2*, 456−465.
(35) Gaus, M.; Cui, Q.; Elstner, M. Density Functional Tight Binding: Application to Organic and Biological Molecules. *WIREs. Comput. Mol. Sci.* **2014**, *4*, 49−61.
(36) Cui, Q.; Elstner, M. Density Functional Tight Binding: Values of Semi-Empirical Methods in an *Ab Initio* Era. *Phys. Chem. Chem. Phys.* **2014**, *16*, 14368−14377.
(37) Henzler-Wildman, K.; Kern, D. Dynamic Personalities of Proteins. *Nature* **2007**, *450*, 964−972.
(38) Kubillus, M.; Kubař, T.; Gaus, M.; Řezáč, J.; Elstner, M. Parameterization of the DFTB3 Method for Br, Ca, Cl, F, I, K, and Na in Organic and Biological Systems. *J. Chem. Theory Comput.* **2015**, *11*, 332−342.
(39) Imoto, T.; Ono, T.; Yamada, H. Binding of Calcium to Lysozyme and Its Derivatives. *J. Biochem.* **1981**, *90*, 335−340.

DOI: 10.1021/acs.jctc.5b00524
J. Chem. Theory Comput. 2015, 11, 4992−5001

(40) Bostrom, M.; Williams, D. R.; Ninham, B. W. Specific Ion Effects: Why the Properties of Lysozyme in Salt Solutions Follow a Hofmeister Series. *Biophys. J.* **2003**, *85*, 686−694.
(41) Machius, M.; Declerck, N.; Huber, R.; Wiegand, G. Activation of Bacillus Licheniformis Alpha-Amylase through a Disorder → Order Transition of the Substrate-Binding Site Mediated by a Calcium−Sodium−Calcium Metal Triad. *Structure* **1998**, *6*, 281−292.
(42) Berman, H. M.; Westbrook, J.; Feng, Z.; Gilliland, G.; Bhat, T. N.; Weissig, H.; Shindyalov, I. N.; Bourne, P. E. The Protein Data Bank. *Nucleic Acids Res.* **2000**, *28*, 235−242.
(43) Phillips, J. C.; Braun, R.; Wang, W.; Gumbart, J.; Tajkhorshid, E.; Villa, E.; Chipot, C.; Skeel, R. D.; Kale, L.; Schulten, K. Scalable Molecular Dynamics with NAMD. *J. Comput. Chem.* **2005**, *26*, 1781−1802.
(44) Dudev, T.; Lim, C. Ion Selectivity Strategies of Sodium Channel Selectivity Filters. *Acc. Chem. Res.* **2014**, *47*, 3580−3587.
(45) MacKerell, A. D.; Feig, M.; Brooks, C. L. Extending the Treatment of Backbone Energetics in Protein Force Fields: Limitations of Gas-Phase Quantum Mechanics in Reproducing Protein Conformational Distributions in Molecular Dynamics Simulations. *J. Comput. Chem.* **2004**, *25*, 1400−1415.
(46) MacKerell, A. D., Jr.; Bashford, D.; Bellott, M.; Dunbrack, R. L., Jr.; Evanseck, J. D.; Field, M. J.; Fischer, S.; Gao, J. a.; Guo, H.; Ha, S. a.; Joseph-McCarthy, D.; Kuchnir, L.; Kuczera, K.; Lau, F. T. K.; Mattos, C.; Michnick, S.; Ngo, T.; Nguyen, D. T.; Prodhom, B.; Reiher, W. E.; Roux, B.; Schlenkrich, M.; Smith, J. C.; Stote, R.; Straub, J.; Watanabe, M.; Wiórkiewicz-Kuczera, J.; Yin, D.; Karplus, M. All-Atom Empirical Potential for Molecular Modeling and Dynamics Studies of Proteins. *J. Phys. Chem. B* **1998**, *102*, 3586−3616.
(47) Best, R. B.; Zhu, X.; Shim, J.; Lopes, P. E. M.; Mittal, J.; Feig, M.; MacKerell, A. D. Optimization of the Additive Charmm All-Atom Protein Force Field Targeting Improved Sampling of the Backbone ϕ, ψ and Side-Chain χ_1 and χ_2 Dihedral Angles. *J. Chem. Theory Comput.* **2012**, *8*, 3257−3273.
(48) Blaudeau, J. P.; McGrath, M. P.; Curtiss, L. A.; Radom, L. Extension of Gaussian-2 (G2) Theory to Molecules Containing Third-Row Atoms K and Ca. *J. Chem. Phys.* **1997**, *107*, 5016−5021.
(49) Mclean, A. D.; Chandler, G. S. Contracted Gaussian-Basis Sets for Molecular Calculations. 1. 2nd Row Atoms, Z = 11−18. *J. Chem. Phys.* **1980**, *72*, 5639−5648.
(50) Raghavachari, K.; Trucks, G. W. Highly Correlated Systems—Excitation-Energies of 1st Row Transition-Metals Sc−Cu. *J. Chem. Phys.* **1989**, *91*, 1062−1065.
(51) Perdew, J. P.; Burke, K.; Ernzerhof, M. Generalized Gradient Approximation Made Simple. *Phys. Rev. Lett.* **1996**, *77*, 3865−3868.
(52) Becke, A. D. Density-Functional Exchange-Energy Approximation with Correct Asymptotic-Behavior. *Phys. Rev. A: At., Mol., Opt. Phys.* **1988**, *38*, 3098−3100.
(53) Perdew, J. P.; Burke, K.; Wang, Y. Generalized Gradient Approximation for the Exchange-Correlation Hole of a Many-Electron System. *Phys. Rev. B: Condens. Matter Mater. Phys.* **1996**, *54*, 16533−16539.
(54) Lee, C. T.; Yang, W. T.; Parr, R. G. Development of the Colle−Salvetti Correlation-Energy Formula into a Functional of the Electron-Density. *Phys. Rev. B: Condens. Matter Mater. Phys.* **1988**, *37*, 785−789.
(55) Miehlich, B.; Savin, A.; Stoll, H.; Preuss, H. Results Obtained with the Correlation-Energy Density Functionals of Becke and Lee, Yang and Parr. *Chem. Phys. Lett.* **1989**, *157*, 200−206.
(56) Tao, J. M.; Perdew, J. P.; Staroverov, V. N.; Scuseria, G. E. Climbing the Density Functional Ladder: Nonempirical Meta-Generalized Gradient Approximation Designed for Molecules and Solids. *Phys. Rev. Lett.* **2003**, *91*, 146401.
(57) Becke, A. D. Density-Functional Thermochemistry. 3. The Role of Exact Exchange. *J. Chem. Phys.* **1993**, *98*, 5648−5652.
(58) Zhao, Y.; Schultz, N. E.; Truhlar, D. G. Design of Density Functionals by Combining the Method of Constraint Satisfaction with Parametrization for Thermochemistry, Thermochemical Kinetics, and Noncovalent Interactions. *J. Chem. Theory Comput.* **2006**, *2*, 364−382.
(59) Schwabe, T.; Grimme, S. Double-Hybrid Density Functionals with Long-Range Dispersion Corrections: Higher Accuracy and Extended Applicability. *Phys. Chem. Chem. Phys.* **2007**, *9*, 3397−3406.
(60) Valiev, M.; et al. Nwchem: A Comprehensive and Scalable Open-Source Solution for Large Scale Molecular Simulations. *Comput. Phys. Commun.* **2010**, *181*, 1477−1489.
(61) Frisch, M.; Trucks, G. W.; Schlegel, H. B.; Scuseria, G. E.; Robb, M. A.; Cheeseman, J. R.; Scalmani, G.; Barone, V.; Mennucci, B.; Petersson, G. A. et al. *Gaussian 09, Revision A.02*; Gaussian, Inc.: Wallingford, CT, 2009.
(62) Sigfridsson, E.; Ryde, U. Comparison of Methods for Deriving Atomic Charges from the Electrostatic Potential and Moments. *J. Comput. Chem.* **1998**, *19*, 377−395.
(63) Singh, U. C.; Kollman, P. A. An Approach to Computing Electrostatic Charges for Molecules. *J. Comput. Chem.* **1984**, *5*, 129−145.
(64) Lu, T.; Chen, F. W. Multiwfn: A Multifunctional Wavefunction Analyzer. *J. Comput. Chem.* **2012**, *33*, 580−592.
(65) Aradi, B.; Hourahine, B.; Frauenheim, T. DFTB+, a Sparse Matrix-Based Implementation of the DFTB Method. *J. Phys. Chem. A* **2007**, *111*, 5678−5684.
(66) Gaus, M.; Goez, A.; Elstner, M. Parametrization and Benchmark of DFTB3 for Organic Molecules. *J. Chem. Theory Comput.* **2013**, *9*, 338−354.
(67) Gaus, M.; Lu, X. Y.; Elstner, M.; Cui, Q. Parameterization of DFTB3/3OB for Sulfur and Phosphorus for Chemical and Biological Applications. *J. Chem. Theory Comput.* **2014**, *10*, 1518−1537.
(68) Curtiss, L. A.; Redfern, P. C.; Raghavachari, K., Gaussian-4 Theory Using Reduced Order Perturbation Theory. *J. Chem. Phys.* **2007**, *127*, 12410510.1063/1.2770701
(69) Kopfer, D. A.; Song, C.; Gruene, T.; Sheldrick, G. M.; Zachariae, U.; de Groot, B. L. Ion Permeation in K^+ Channels Occurs by Direct Coulomb Knock-On. *Science* **2014**, *346*, 352−355.
(70) Wheatley, R. W.; Juers, D. H.; Lev, B. B.; Huber, R. E.; Noskov, S. Y. Elucidating Factors Important for Monovalent Cation Selectivity in Enzymes: *E. coli* Beta-Galactosidase as a Model. *Phys. Chem. Chem. Phys.* **2015**, *17*, 10899−10909.
(71) Mildvan, A. S.; Xia, Z.; Azurmendi, H. F.; Saraswat, V.; Legler, P. M.; Massiah, M. A.; Gabelli, S. B.; Bianchet, M. A.; Kang, L. W.; Amzel, L. M. Structures and Mechanisms of Nudix Hydrolases. *Arch. Biochem. Biophys.* **2005**, *433*, 129−43.
(72) Dudev, T.; Lin, Y. L.; Dudev, M.; Lim, C. First-Second Shell Interactions in Metal Binding Sites in Proteins: A PDB Survey and DFT/CDM Calculations. *J. Am. Chem. Soc.* **2003**, *125*, 3168−3180.
(73) Capozzi, F.; Ciurli, S.; Luchinat, C. Coordination Sphere Versus Protein Environment as Determinants of Electronic and Functional Properties of Iron-Sulfur Proteins. *Struct. Bonding* **1998**, *90*, 127−160.
(74) Carmona, U.; Li, L.; Zhang, L. B.; Knez, M. Ferritin Light-Chain Subunits: Key Elements for the Electron Transfer across the Protein Cage. *Chem. Commun.* **2014**, *50*, 15358−15361.
(75) Cwiklik, L.; Buck, U.; Kulig, W.; Kubisiak, P.; Jungwirth, P. A Sodium Atom in a Large Water Cluster: Electron Delocalization and Infrared Spectra. *J. Chem. Phys.* **2008**, *128*, 154306.
(76) Slavíček, P.; Roeselova, M.; Jungwirth, P.; Schmidt, B. Preference of Cluster Isomers as a Result of Quantum Delocalization: Potential Energy Surfaces and Intermolecular Vibrational States of Ne···HBr, Ne···HI, and $HI(Ar)_{(n)}$ (n = 1−6). *J. Chem. Phys.* **2001**, *114*, 1539−1548.
(77) Gresh, N. Development, Validation, and Applications of Anisotropic Polarizable Molecular Mechanics to Study Ligand and Drug-Receptor Interactions. *Curr. Pharm. Des.* **2006**, *12*, 2121−2158.

DOI: 10.1021/acs.jctc.5b00524
J. Chem. Theory Comput. 2015, 11, 4992−5001